

Supporting Information

for

The role of L-Cysteine and introduced surface defects in reactive oxygen species generation by ZnO nanoparticles

Dominika Wawrzyńczyk^{1,*}, Bartłomiej Cichy², Wiesław Stręk²
and Marcin Nyk¹

¹ *Advanced Materials Engineering and Modelling Group, Faculty of Chemistry, Wrocław University of Technology, Wybrzeże Wyspiańskiego 27, 50-370 Wrocław, Poland*

² *Institute of Low Temperature and Structure Research, PAS, Okólna 2, 50-422 Wrocław, Poland*

* corresponding author: dominika.wawrzynczyk@pwr.edu.pl

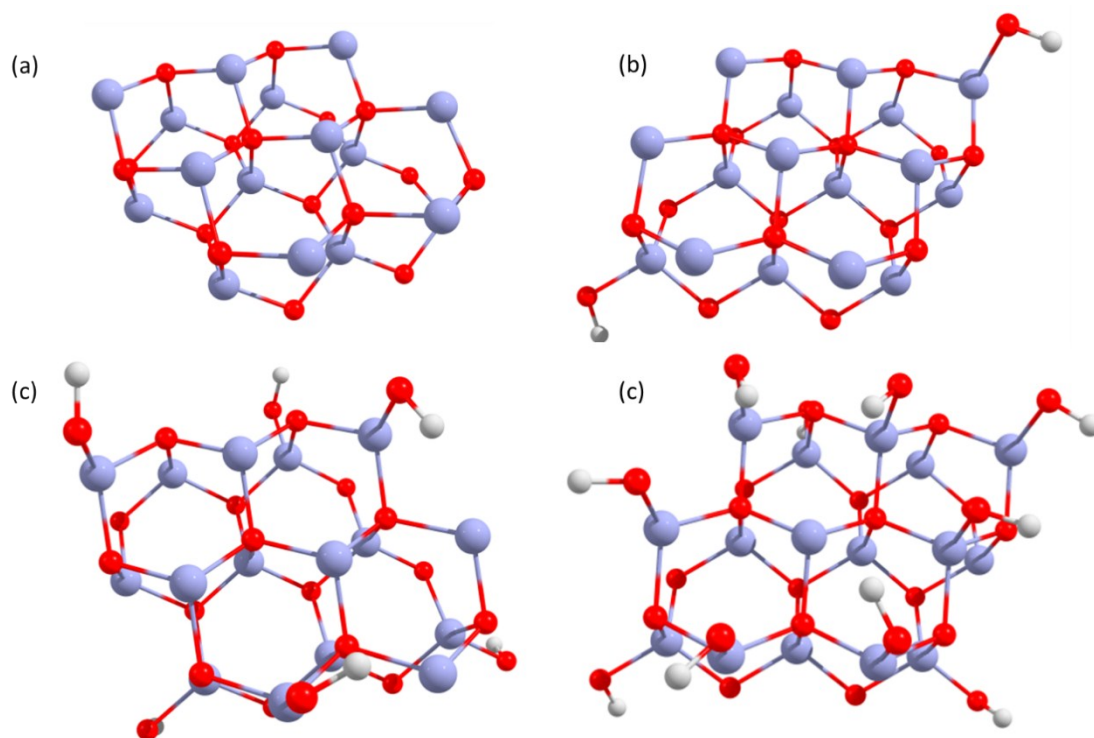


Figure S1 Unoptimized geometries of the Zn₁₆O₁₆ clusters with the (a) 0, (b) 2, (c) 6 and (d) 10 OH groups adhered to the cluster's surface.

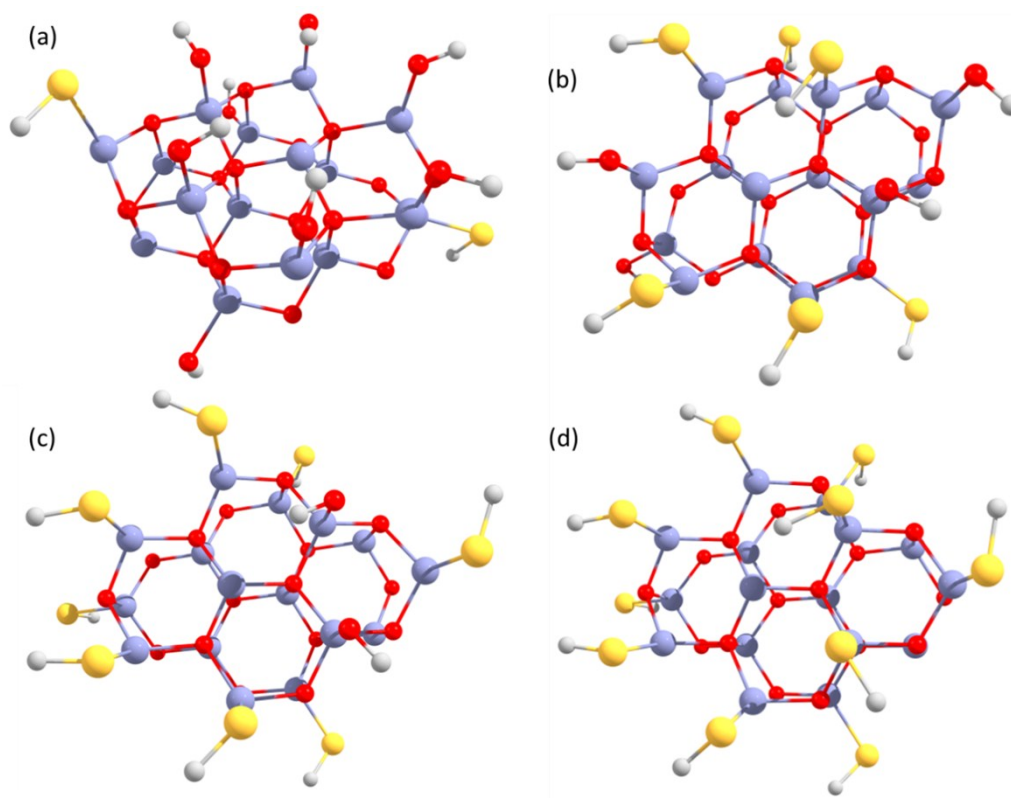


Figure S2 The unoptimized geometries of the $\text{Zn}_{16}\text{O}_{16}$ clusters with the (a) 2xSH, 8xOH (b) 6xSH, 4xOH (c) 8xSH, 2xOH and (d) 10 SH groups adhered to the cluster's surface.

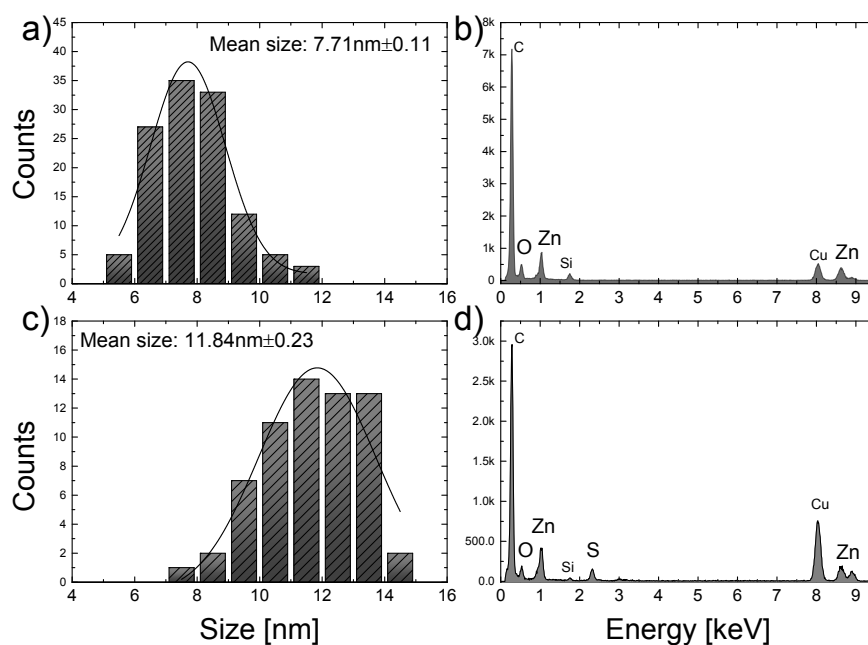


Figure S3 Size distribution histograms of as-synthesized raw-ZnO NPs (a) and after surface functionalization with L-Cysteine molecules (2 mmol) (c) calculated based on TEM images, together with EDS spectrum before (b) and after (d) surface functionalization.

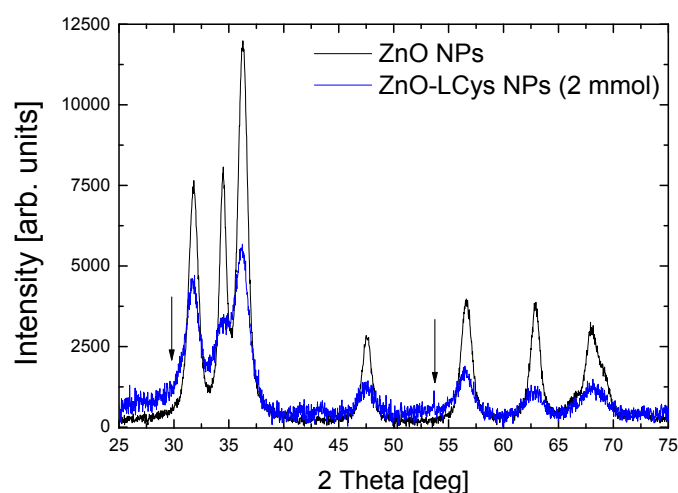


Figure S4 XRD patterns of as synthesized ZnO NPs powder (black) and the powder obtained after drying a dispersion of ZnO-LCys NPs (blue).

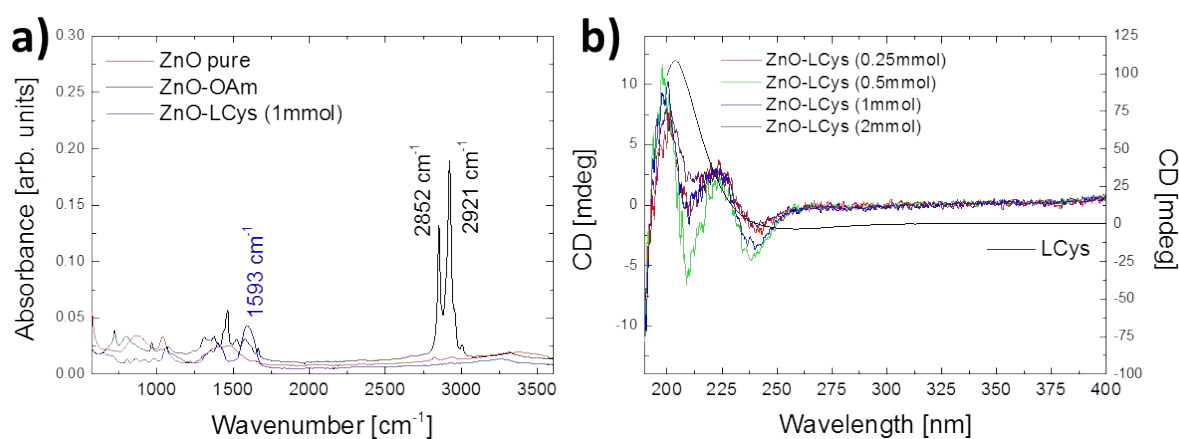


Figure S5 Representative FTIR spectra of ZnO NPs before and after surface functionalization with L-Cysteine and Oleylamine molecules (a), and CD spectra of L-Cysteine functionalized ZnO NPs compared to the spectra of pure L-Cysteine molecules in water.

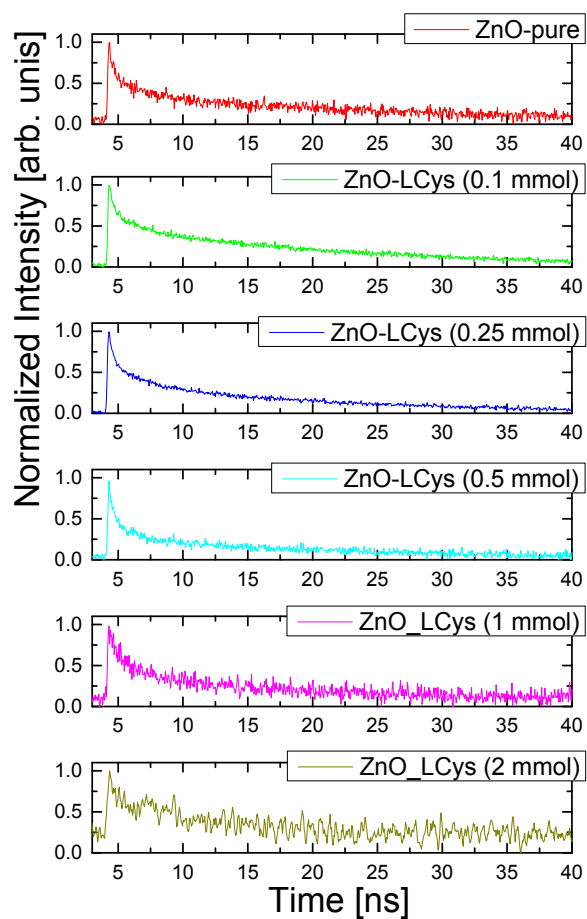


Figure S6 Luminescence decays curves for visible ($\lambda_{EM}=540$ nm) emission in ZnO NPs functionalized with different amounts of L-Cys molecules.

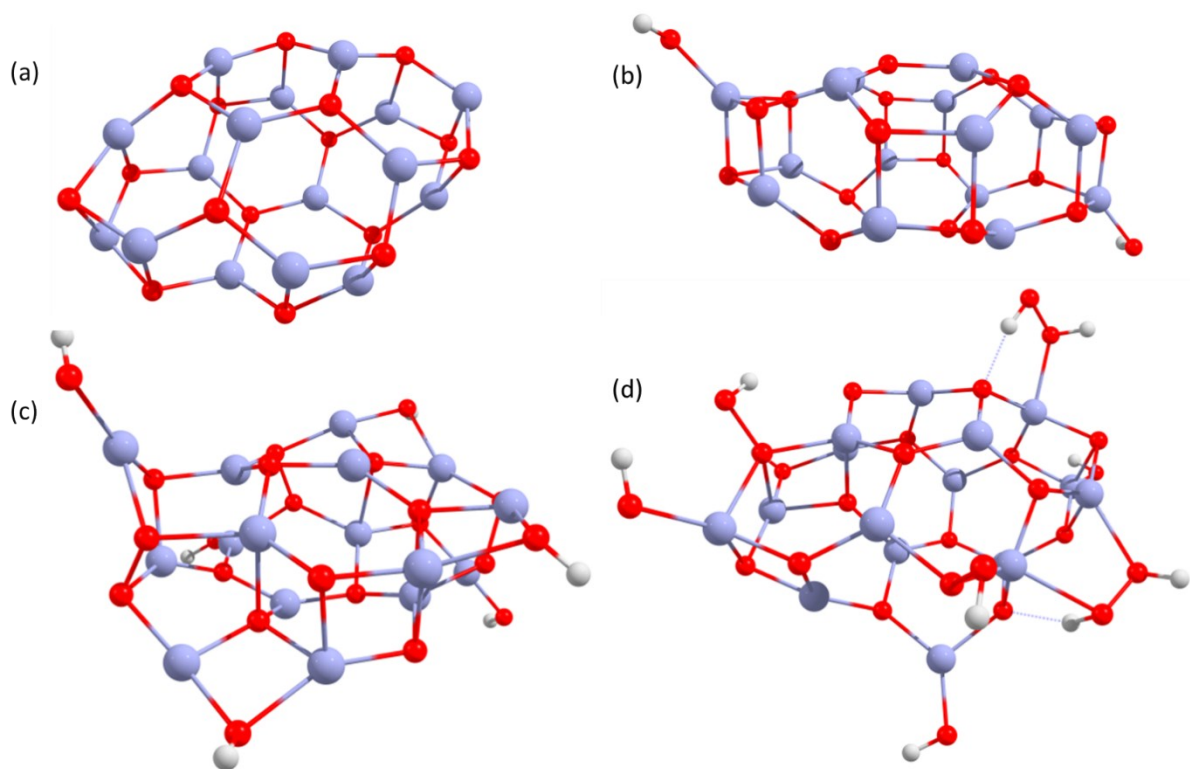


Figure S7 The stationary point geometries of the Zn₁₆O₁₆ clusters with the (a) 0, (b) 2, (c) 6 and (d) 10 OH groups adhered to the cluster's surface.

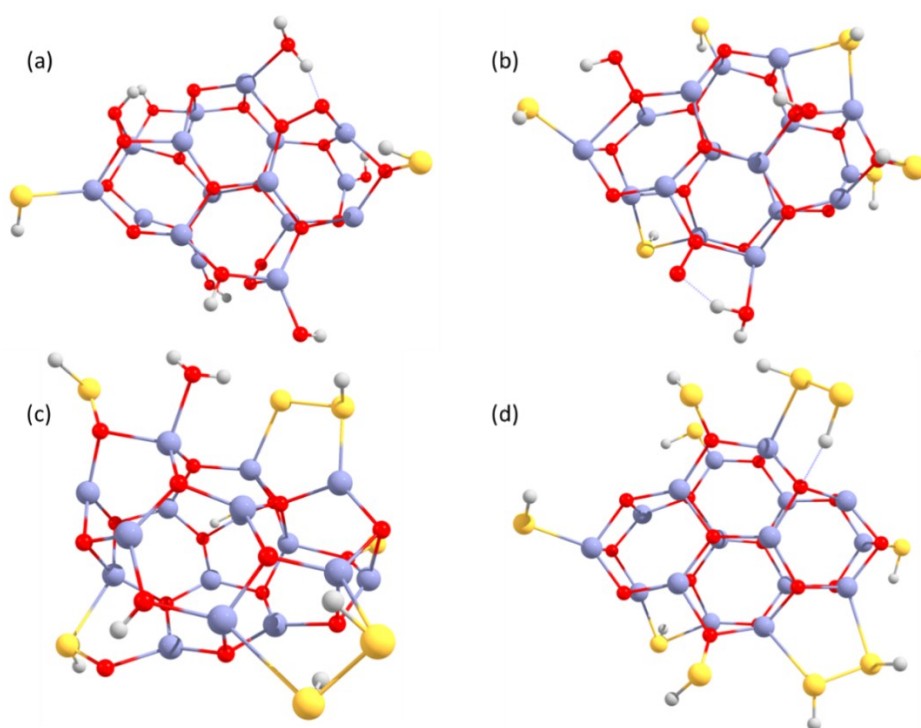


Figure S8 The stationary point geometries of the Zn₁₆O₁₆ clusters with the (a) 2xSH, 8xOH (b) 6xSH, 4xOH (c) 8xSH, 2xOH and (d) 10 SH groups adhered to the cluster's surface.

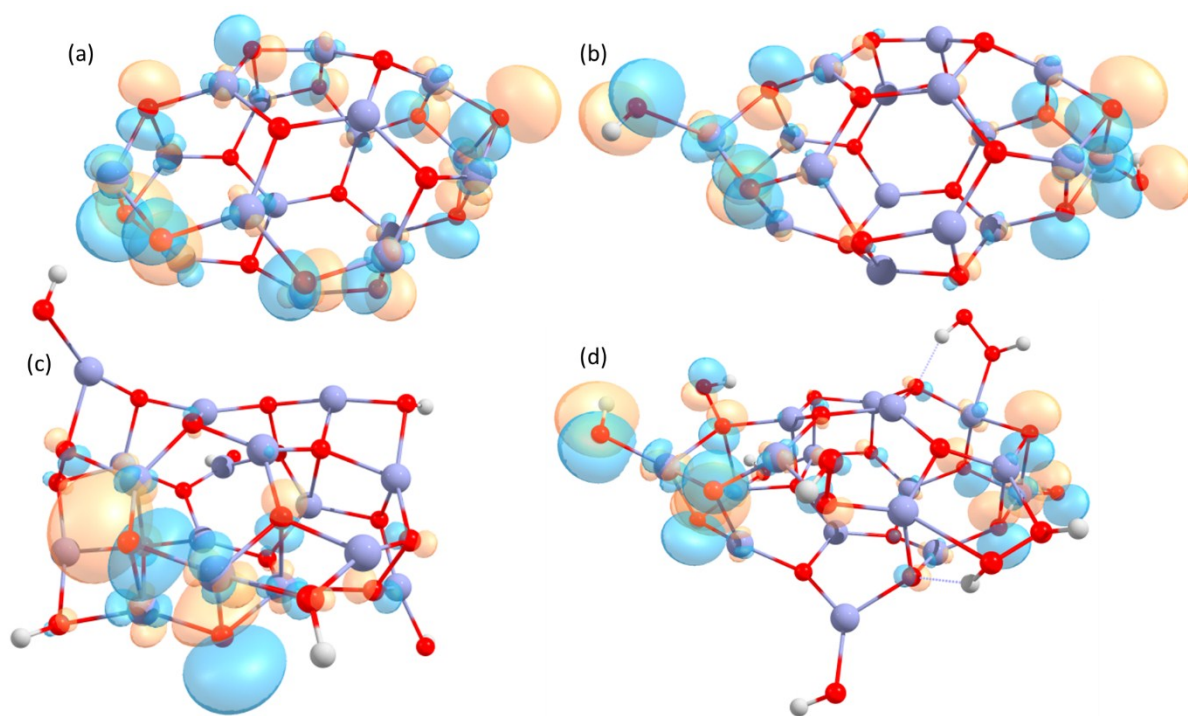


Figure S9 The stationary point geometries of the $\text{Zn}_{16}\text{O}_{16}$ clusters with various number of the OH groups attached to the surface i.e. (a) $0\times\text{OH}$, (b) $2\times\text{OH}$, (c) $8\times\text{OH}$ and (d) $10\times\text{OH}$. The HOMO orbitals are shown for each optimized structure.

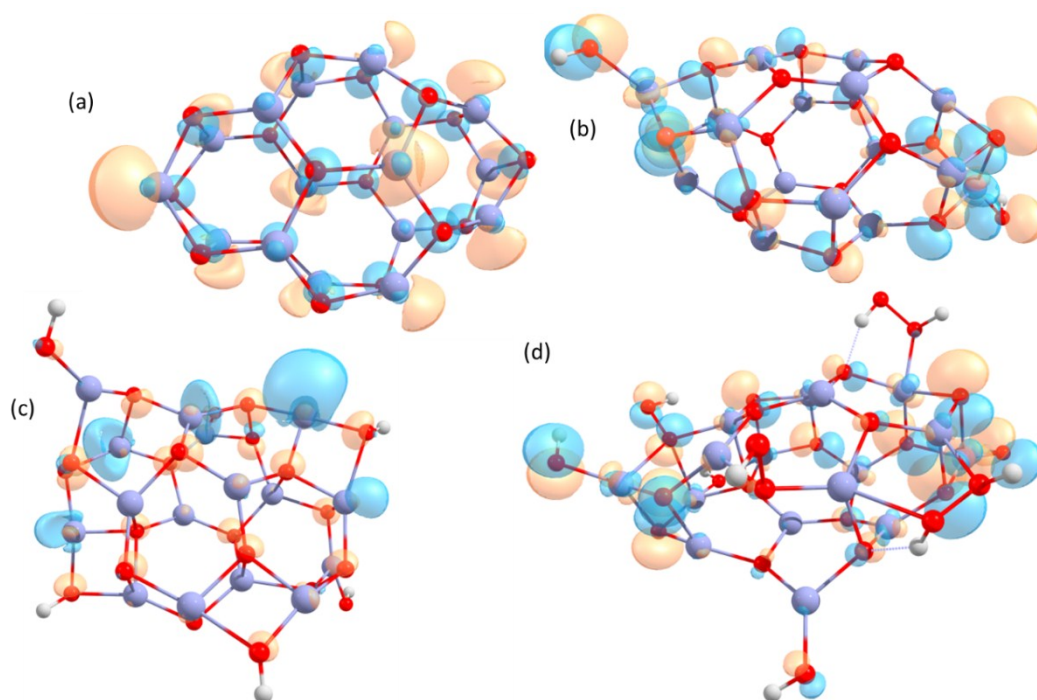


Figure S10 The stationary point geometries of the $\text{Zn}_{16}\text{O}_{16}$ clusters with various number of the OH groups attached to the surface i.e. (a) $0\times\text{OH}$, (b) $2\times\text{OH}$, (c) $8\times\text{OH}$ and (d) $10\times\text{OH}$. The LUMO orbitals are shown for each optimized structure.

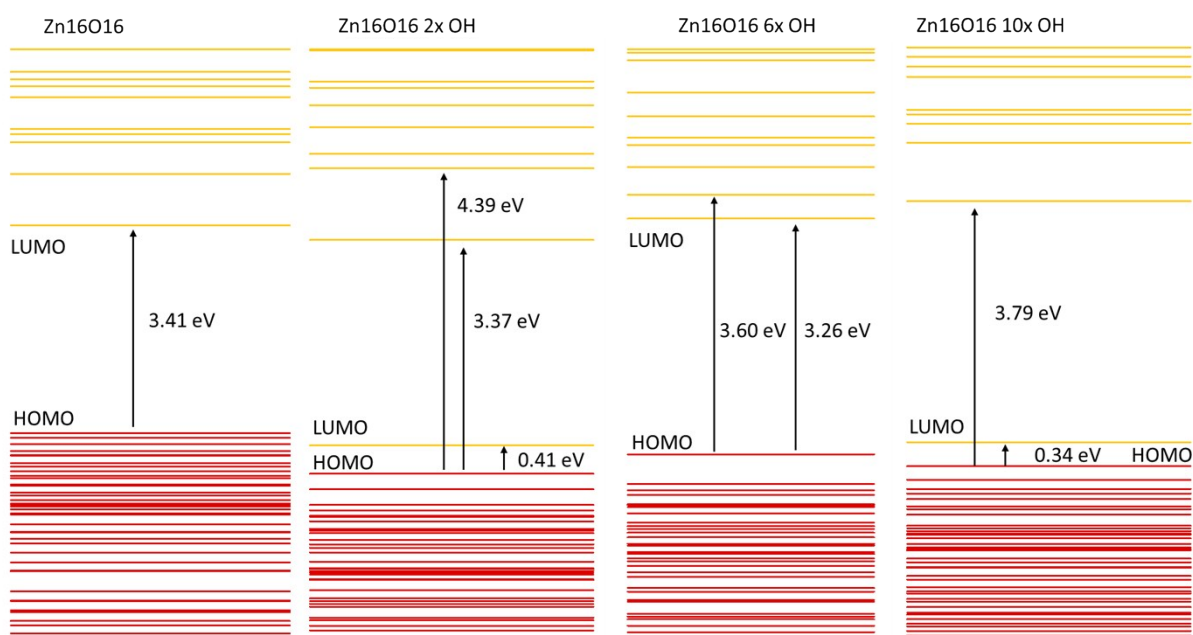


Figure S11 The energy diagrams for the $\text{Zn}_{16}\text{O}_{16}$ clusters with various number of the OH groups attached to the surface i.e. (a) 0xOH, (b) 2xOH, (c) 8xOH and (d) 10xOH.

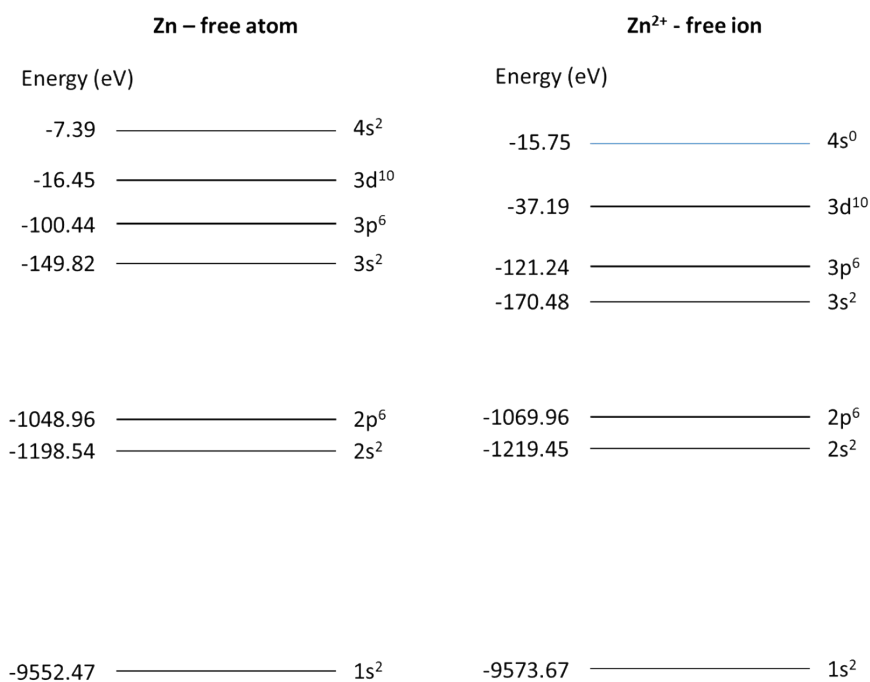


Figure S12 The energies of the atomic orbitals calculated for the (a) neutral Zn atom and the (b) free Zn^{2+} ion. The first virtual orbital was related to the 4s state has been colored in blue.

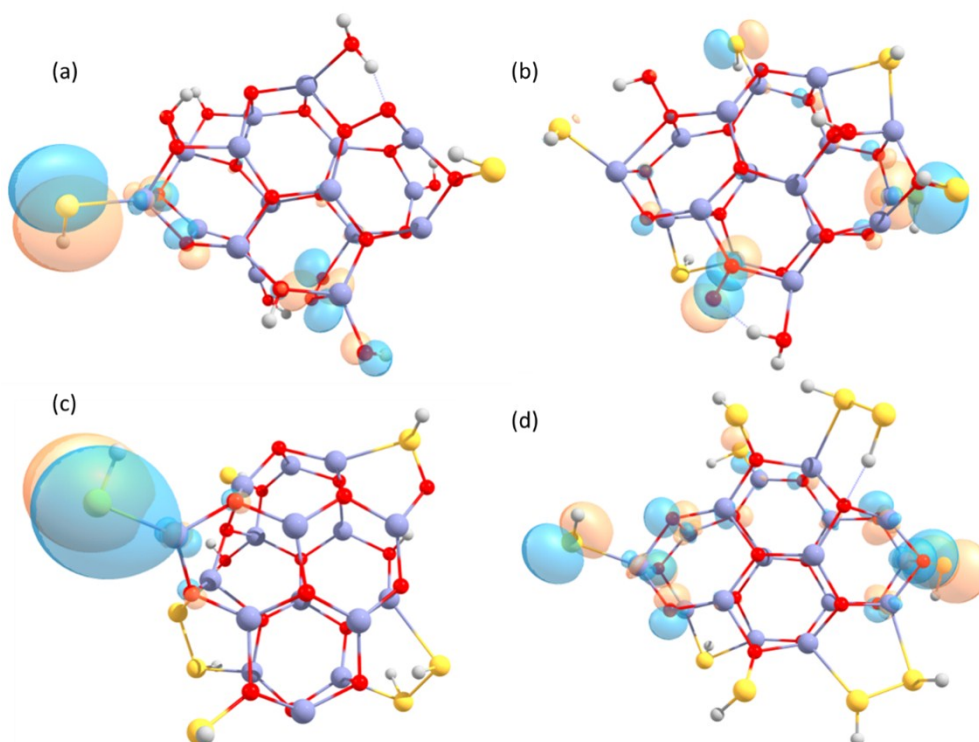


Figure S13 The stationary point geometries of the $\text{Zn}_{16}\text{O}_{16}$ clusters with the (a) 2xSH, 8xOH (b) 6xSH, 4xOH (c) 8xSH, 2xOH and (d) 10 SH groups adhered to the cluster's surface. HOMO orbitals has been depicted.

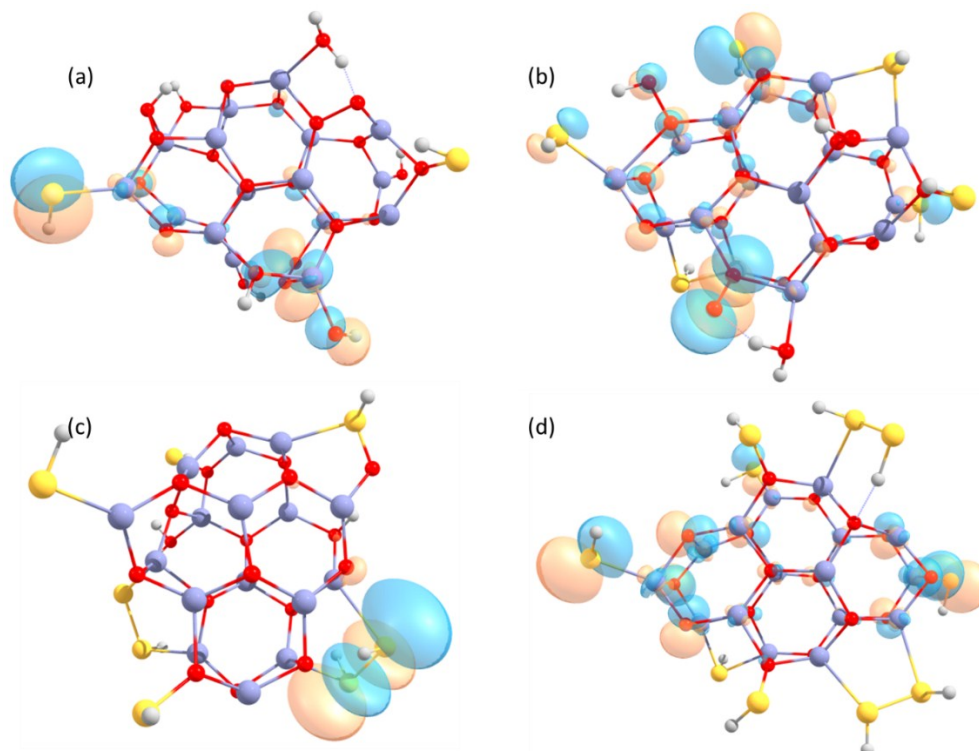


Figure S14 The stationary point geometries of the $\text{Zn}_{16}\text{O}_{16}$ clusters with the (a) 2xSH, 8xOH (b) 6xSH, 4xOH (c) 8xSH, 2xOH and (d) 10 SH groups adhered to the cluster's surface. HOMO orbitals has been depicted.

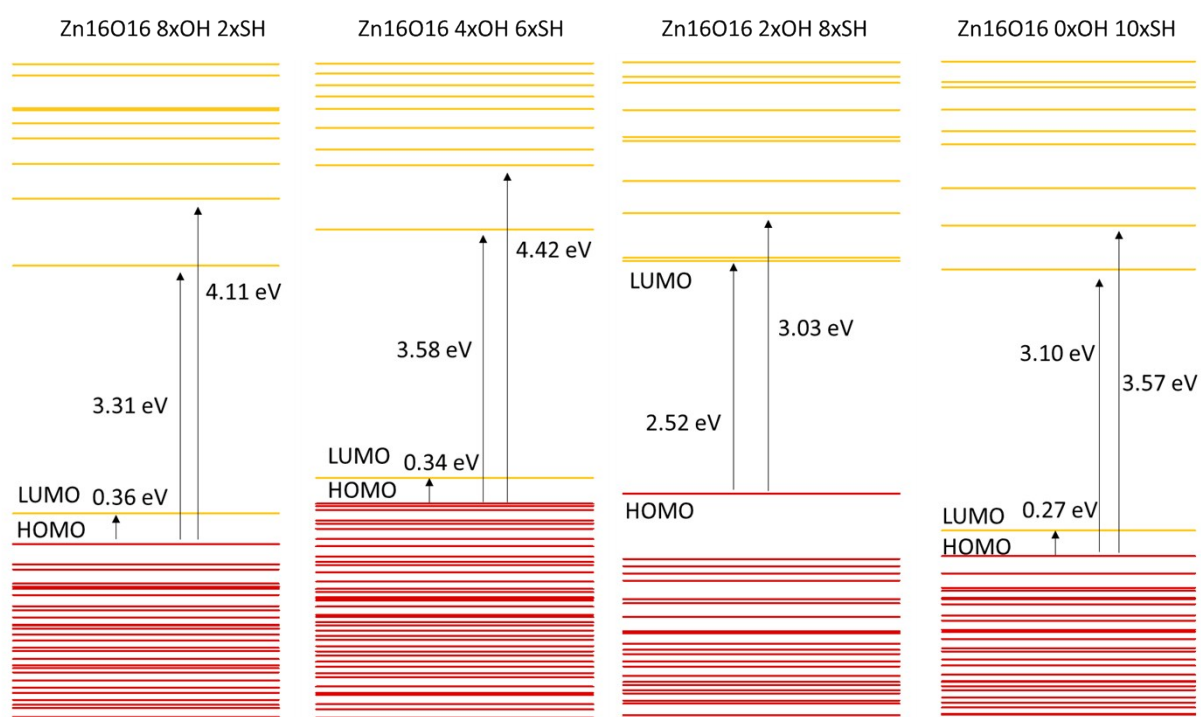


Figure S15 The energy diagrams for the $\text{Zn}_{16}\text{O}_{16}$ clusters modified by the (a) 2xSH, 8xOH (b) 6xSH, 4xOH (c) 8xSH, 2xOH and (d) 10 SH groups adhered to the cluster's surface.